Journal Pre-proofs

Structural evolution, electronic and magnetic properties investigation of $V_3Si_n^-$ (n=14–18) clusters based on photoelectron spectroscopy and density functional theory calculations

Kai Wang, Guang-Jia Yin, Ze-Zhao Jia, Lin Miao, Hong-Yuan Zhao, Ramiro Moro, Bernd von Issendorff, Lei Ma

PII: S0009-2614(23)00128-8
DOI: https://doi.org/10.1016/j.cplett.2023.140423
Reference: CPLETT 140423

To appear in: *Chemical Physics Letters*

Received Date: 13 November 2022
Revised Date: 1 February 2023
Accepted Date: 7 March 2023

Please cite this article as: K. Wang, G-J. Yin, Z-Z. Jia, L. Miao, H-Y. Zhao, R. Moro, B. von Issendorff, L. Ma, Structural evolution, electronic and magnetic properties investigation of $V_3Si_n^-$ (n=14–18) clusters based on photoelectron spectroscopy and density functional theory calculations, *Chemical Physics Letters* (2023), doi: https://doi.org/10.1016/j.cplett.2023.140423

Structural evolution, electronic and magnetic properties investigation of $V_3Si_n^-$ (n=14–18) clusters based on photoelectron spectroscopy and density functional theory calculations

Kai Wang, [1,§] Guang-Jia Yin,[2,§] Ze-Zhao Jia, [1] Lin Miao, [1] Hong-Yuan Zhao, [1] Ramiro Moro, [1]Bernd von Issendorff, [2] and Lei Ma[1,*]

[1]Tianjin International Center for Nanoparticles and Nanosystems, Tianjin University, 92 Weijin Road, Nankai District, Tianjin 300072, China

[2]Fakultät für Physik, Universität Freiburg, H. Herderstr. 3. D-79104 Freiburg, Germany

*Authors to whom correspondence should be addressed: lei.ma@tju.edu.cn

[§]K. W. and G.J. Y. contributed equally to this paper.

ABSTRACT: Silicon clusters doped with a transition metal (TM) atom have been intensively studied due to their novel properties and superior stability for possible usage as building blocks of future nanoelectronics. Besides the selection of the doped element, introducing the number of dopant atoms as another dimension adds versatility to tuning the cluster properties. However, there are few studies of silicon clusters doped with multiple TM atoms. Here, we present a study of $V_3Si_n^-$ (n=14–18) by combining high-resolution photoelectron spectroscopy (PES) measurements with a search of their global minimum energy structures based on a homemade genetic algorithm coupled with density functional theory (DFT) for energy calculations. The simulated photoelectron spectra of the putative global minimum structures are in fair agreement with the experimental ones, which gives evidence for their authenticity as the ground-state structures. In these clusters the three V atoms always bond with each other and form an acute triangle, which can be seen as a nanoscale analogue of phase segregation in the bulk. For the size range n=14–17, each of the ground-state structures has a silicon basket-like structure with the vanadium triangle inside, while $V_3Si_{18}^-$ has a baseball-mitt-like structure almost completely encapsulating the V_3 triangle. The average binding energy of $TMSi_n^-$ (TM= V_1, V_2, V_3) indicates that the

more V atoms are doped the more stable the clusters are. Among these clusters, only $V_3Si_{14}^-$ have a total magnetic moment of 2 μ_B, making it a potential structural unit for magnetic storage devices. Mulliken population analysis and the electron spin density show that V atoms at different positions have different contributions to the total magnetic moments, and d electrons in V atoms contribute the most.

1. INTRODUCTION

Being the embryos of bulk silicon (Si), Si clusters have been extensively investigated owing to their potential applications in the next generation of microelectronic devices.[1-9] Due to their chemical reactivity, [1,10-12] the transition metal (TM) doped Si clusters have attracted great attention since such doping may enhance their stability and bring novel physical properties.[13-18]

A large number of experimental and theoretical studies have been reported on the geometric structures and physical properties of single TM atom doped Si_n clusters. For example, the electronic properties of $CrSi_{8-12}^-$,[20] TM-Si_{6-20}^- (TM= Sc, Ti, V, Y, Zr, Nb, Hf, Ta),[19] MSi_{16}^- (M = Sc, Ti, V, Y, Zr, Nb, Lu, Hf, Ta)[16] and MSi_{16}^- (M =Sc, Ti, V)[15] have been studied by PES. The stability of TM (Cr, Mn, Cu, Mo, W)-doped Si clusters has been investigated through mass spectrum (MS) experiments, showing that $CrSi_{15,16}^+$, $MnSi_{15,16}^+$, and $CuSi_{6,10}^+$ are especially stable.[17] Similarly, MS also shows that MSi_{16} (M = Sc^-, Ti, V^+, Y^-, Zr, Nb^+, Lu^-, Hf and Ta^+) have high stabilities due to their closed geometric and electronic configurations.[15, 16] Besides the experimental efforts, intensive theoretical studies on the structures and electronic properties of $TiSi_{2-15}$,[21] $CrSi_{8-17}^-$,[22] $Si_{14-17}M$ (M=Cr, Mo, and W),[23] $Si_{14-18}M$ (M=Sc^-, Ti, V^+),[24] $FeSi_{2-14}$,[25] $CoSi_{1-13}$ [26] and $NiSi_{1-8}$ [27] also have been conducted. The direct combination of experiments and theoretical calculations has proven to be especially fruitful. A series of single-TM-doped (TM = V, Cr, Cu, Nb, Ag) Si_n^- (n≤18) clusters were systematically studied based on combining PES and DFT calculations, whereby many structures and properties have been unveiled.[28-34]

The selection of the doping element is one factor to stabilize and tune the properties of these mixed clusters. Doping with several atoms introduces the number of dopants as another dimension to tailor the desired properties. This also opens more questions such as about their geometric structures, how the stability is affected, whether the dopants are segregated or separated in the cluster and how the chemical properties vary due to resulting HOMO-LUMO gap changes. More importantly, these studies also open an avenue to gain insight into the early growth stages of bulk alloys. Therefore, it is of special interest to explore the structures and properties of multi-TM-atom doped Si clusters.

As discussed above, comprehensive studies have been dedicated to Si_n clusters with a single TM atom dopant, whereas only few works have focused on clusters with multi-TM-atom dopants. Systems such as $V_mSi_n^-$ (m=1–2, n=3–6)[35] , $V_2Si_n^-$ (n=1–10)[36], $Sc_2Si_x^-$(x=2–6)[37], and $TMSi_n^-$ (TM=V_2,Cr_2; n=14–20)[38] were studied, revealing the existence of a strong V–V interaction and weak Sc–Sc interaction in those clusters. They also show that V_2Si_{20} adopts a fullerene-like Si_{20} cage as the structural motif with the vanadium dimer encapsulated inside.[39] Another study predicted that both $Cr_2Si_{13}^-$ and $Cr_3Si_{12}^-$ possess large magnetic moments of $3\mu_B$ and $7\mu_B$, respectively.[40] It has also been reported that $V_3Si_{12}^-$ has a surprisingly large magnetic moment of $4\mu_B$.[41] To the best of our knowledge, there are just three published studies about small size Si_n clusters doped with three TM atoms ($V_3Si_{12}^-$,[41] $V_3Si_{3-14}^-$,[42] and $Cr_3Si_{12}^-$ [40]), while larger sizes (n>14) have not been explored yet. This might be due to the lack of experimental data and the great challenge of determining the global minimum geometries, given the huge amount of possible isomer structures for multiple TM atoms and a large number of Si atoms).

Here, experimental PES and DFT calculations were carried out to explore the structural evolution and electronic properties of $V_3Si_n^-$ in the size range n =14–18. The authenticity of the found ground state structures was justified by the reasonable agreement between the simulated PESs and the measured ones. The electronic structures and growth patterns are discussed systematically. It was found that the V atoms tend to segregate forming the core of the cluster and that the cluster stabilities are superior to those of pure silicon clusters.

2. EXPERIMENTAL AND THEORETICAL METHODS

2.1. Experimental methods

The experiments were performed employing a magnetic-bottle PES apparatus equipped with a magnetron sputtering gas aggregation cluster source, which has been described in detail elsewhere.[9,32,33,38,43] In brief, V and Si atoms were sputtered from a sandwiched VSi target by a magnetically confined plasma into a liquid nitrogen cooled aggregation tube filled with a mixture of the carrier gases helium and argon (ratio 3:1) under a total pressure of about 0.5 mbar, where V and Si atoms aggregate into clusters. Then, after expansion into the vacuum, the clusters were fed into a radio-frequency 12-pole cryogenic ion trap cooled down to 10 K. In this trap the clusters were thermalized by collisions with helium buffer gas under a pressure of around 10^{-3} mbar. The V-doped Si clusters were extracted collinearly forming cluster bunches and analyzed by a high-resolution, double reflection time-of-flight mass spectrometer. A given cluster size was selected by a multi-wire mass gate in between the two reflectors with a resolution of about m/Δm=2000, before being decelerated

and photodetached by a 248 nm KrF laser for the PES acquisition in the interaction region of the photoelectron spectrometer. Photoelectron spectra s were typically averaged over 30000 laser shots at a repetition rate of 100 Hz; calibration using the PES of Pt^- under the same conditions ensured measured binding energy uncertainties of smaller than 30 meV.

2.2. Theoretical methods

In order to get global minimum (GM) structures, the global search was conducted through a homemade genetic algorithm code[32,33,38,44,45] interfaced to the ORCA program[46,47] for energy calculations. During the searching process, the BP86 functional[48] and def2-SVP basis set[49,50] were employed to optimize the isomers generated from the searching code. For each cluster size, more than 3000 configurations were generated to assure a high chance of locating the global minimum on the potential energy surface. The top 10-30 low-energy isomers were further optimized by using def2-TZVP basis set to acquire more accurate structures. The diffuse def2-TZVP (def2-TZVPD)[51] basis set was adopted to acquire electronic energies with higher accuracy. All the structures have no imaginary frequencies from the vibration analyses results. Zero-point-energy (ZPE) corrections were included for the relative energy calculations. Among all the tested functionals (see supplementary materials), including PBE,[52] BLYP,[53,54] PBE0,[55] TPSS,[56] TPSSh,[57] and B3P[58], BP86 yields vertical detachment energies (VDEs) and electronic density of states of the lowest-lying isomers of $V_3Si_n^-$ (n=14−18) closest to the measured ones.

The first VDE was calculated as the total energy difference between the anionic and the neutral cluster, both within the relaxed geometric structure of the anion. In order to directly compare with the experimental spectra, each line of the Kohn–Sham (KS) eigenvalue spectrum was broadened by convolution with a Gaussian function with a width of 0.06 eV to yield the simulated density of states (DOS). Then, the spectra were shifted by the difference of the VDE and highest-occupied KS orbital (HOMO) energy to generate simulated PES according to the generalized Koopmans' theorem.[59] The graphs of the $V_3Si_n^-$ (n=14−18) clusters were rendered by using Visual Molecular Dynamics (VMD) software.[60] The electron spin density and population analysis were performed with the Multiwfn 3.8 (dev)[61] based on the output results of the ORCA program. Considering that the Mulliken population analysis is very sensitive to the diffuse basis set, therefore, the population analysis is performed at the BP86/def2-TZVP level.

3. RESULTS AND DISCUSSIONS

3.1. The photoelectron spectra of $V_3Si_n^-$ (n =14−18)

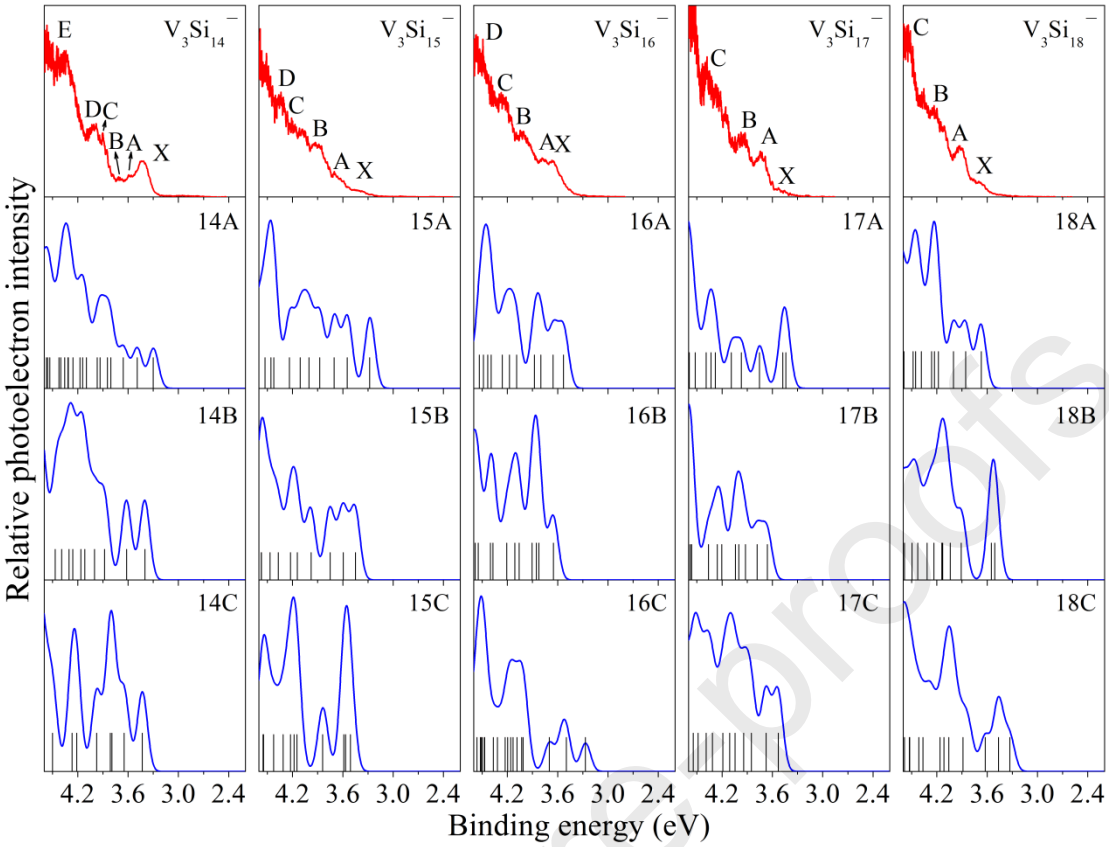

Figure 1. Uppermost panels: experimental PES spectra of cold $V_3Si_n^-$ (n = 14–18), measured at a photon energy of 5.0 eV. Lower panels: theoretical PES spectra, calculated by density functional theory at the BP86/def2-TZVPD level for the structures shown in Figure 2.

The measured photoelectron spectra for the $V_3Si_n^-$ (n=14−18) clusters are shown together with the simulated spectra of the putative global minimum structures in Figure 1. In the experimental PES, each spectrum has several peaks labeled as X and A to E. The X peak represents the electron detachment transition from the anionic ground state to that of neutral cluster, whereas the higher energy peaks, A to E, denote the detachment transitions to the excited states of the neutral species. The VDEs for the first observed peaks are listed in Table 2, in comparison with the calculated ones.

There are three main peaks (X, D, and E) in the PES of $V_3Si_{14}^-$, centered at 3.40 eV, 3.90 eV and 4.33 eV. Moreover, there are two slightly smeared small peaks at the bottom of the valley between peaks X and C, and a peak D next to the main peak E. The measured spectrum of $V_3Si_{15}^-$ is several ripples sitting on a ramping slope, from which we can see five barely resolved peaks, located at 3.38 eV, 3.69 eV, 3.95 eV, 4.15 eV and 4.34 eV. For $V_3Si_{16}^-$, the peaks X and A are partially overlapping,

centered at 3.65 eV and 3.78 eV, followed by two well resolved peaks B and C and a large band, centered at 4.00 eV, 4.30 eV and 4.60 eV, respectively. The PES of $V_3Si_{17}^-$ has a smeared weak peak X centered at 3.53 eV, a well resolved A peak centered at 3.70 eV, a B peak centered at 3.95 eV, and a broad peak C centered at 4.40 eV. Similar to $V_3Si_{17}^-$, the spectrum of $V_3Si_{18}^-$ has three resolvable peaks X, A, and C, and a band B located at 3.70 eV, 3.94 eV, 4.55 eV, and 4.2 eV, respectively.

In order to obtain more information, lowest energy structures of these clusters have been searched globally, and the results are shown in Figure 2. The relative energies of these isomers are given in Table 2. The calculated photoelectron spectra of these structures are compared to the measured ones in Figure 1; more isomers and simulated spectra are displayed in the Supplementary Materials. In general, the main features of the measured spectra for these $V_3Si_n^-$ clusters are reproduced by the calculations for the lowest energy structures, which evidences that the correct ground state structures of these clusters have been found.

3.2. Structures of the $V_3Si_n^-$ (n =14−18) clusters

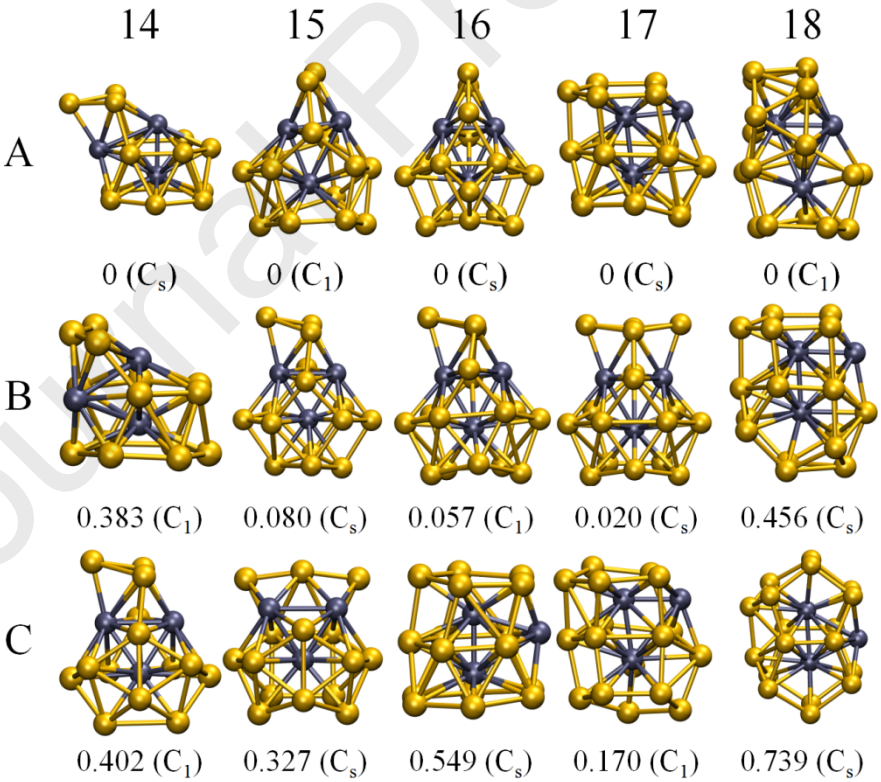

Figure 2. Low-lying structures of $V_3Si_n^-$ (n = 14−18) clusters with symmetries given in parenthesis. They are marked with nA, nB, and nC ordered by energy (eV). Grey and yellow balls represent V and Si atoms, respectively.

Figure 2 shows the low-lying structures of $V_3Si_n^-$ (n=14−18) clusters optimized at the BP86/def2-TZVP level. For size n=14, the lowest-energy structure can be viewed as a V_3 triangle inserted into a Si hexagonal prism, forming a V_2 axle and substituting one Si atom on the top hexagon with a V atom. The other three Si atoms form a halo-like triangle above this V atom substitute. This structure is consistent with an earlier report.[42] Nevertheless, our calculation shows that 14A is not in a singlet state as stated in that report,[42] but in a triplet state, which is lower in energy by 0.051 eV than the singlet at the BP86/def2-TZVPD level. The structure of isomer 14B can be obtained by reconstruction of the upper three silicon atoms in 14A, resulting in C_1 symmetry. The isomer 14C can be viewed as a basket-like Si_{11} with an inserted V_3 triangle and three extra silicon atoms attached on the top. The lowest-energy structure of $V_3Si_{15}^-$, can be constructed by inserting a V_3 triangle into a severely distorted heptagon-hexagon basket with two Si atoms forming a handle-like structure in C_1 symmetry. Isomers 15B and 15C also adopt a similar Si_{12} basket-like structure with a V_3 triangle inserted and with three silicon atoms added on top. The lowest-energy structure of $V_3Si_{16}^-$ can be viewed as a basket-like Si_{15} structure with a silicon atom attached on the surface and a V_3 triangle inserted inside. Isomer 16B has a Si_{13} basket-like shape with three Si atoms forming a triangle like handle and the V_3 triangle inside, overall showing C_1 symmetry. The isomer 16C can be seen as a Si_{16} cylindrical cage with a partially embedded V_3 triangle having one exposed V atom. For $V_3Si_{17}^-$, both 17A and 17C can be regarded as grown from 16C. Isomer 17B can be obtained by adding a Si atom to the top of the isomer 16B. In $V_3Si_{18}^-$, the lowest-energy structure can be viewed as a Si_{18} baseball-mitt-like structure catching a V_3 triangle with only one exposed V atom. The isomer 18B can be regarded as a distorted and extended version of 17A. The isomer 18C can be seen as a V_3 triangle embedded in a Si_{18} cage with one exposed V atom.

Table 1. The average V–Si, Si–Si, and V–V bond lengths of the lowest-energy structures of $V_3Si_{14\text{-}18}^-$ clusters based on BP86/def2-TZVP optimization. $r_{V–Si}$ and $r_{Si–Si}$ are the average V–Si and Si–Si bond lengths, and $r_{max\_V\text{-}V}$, $r_{mid\_V–V}$ and $r_{min\_V\text{-}V}$ are the maximum, middle and minimum V–V bond lengths, respectively.

Cluster	Bond length (Å)				
	$r_{V–Si}$	$r_{Si–Si}$	$r_{max\_V\text{-}V}$	$r_{mid\_V–V}$	$r_{min\_V\text{-}V}$
$V_3Si_{14}^-$	2.60	2.47	2.99	2.90	2.32
$V_3Si_{15}^-$	2.65	2.40	2.96	2.47	2.25
$V_3Si_{16}^-$	2.67	2.42	2.60	2.59	2.26
$V_3Si_{17}^-$	2.64	2.49	3.29	2.38	2.32
$V_3Si_{18}^-$	2.63	2.51	2.85	2.82	2.29

In all cases, vanadium atoms form an acute triangle within the cluster which is consistent with smaller sizes of $V_3Si_{3\text{-}14}^-$ reported previously.[42] In the ground-state structures of $V_3Si_{3-14}^-$, when the size is less than 11, all three V atoms are exposed, while for larger sizes, one of the three V atoms is embedded inside the cluster.[42] As illustrated in Figure 2, for the size of $14 \le n \le 17$, the lowest-energy structures of $V_3Si_n^-$ always have two exposed V atoms, while there is only one exposed V atom in the lowest-energy structure of $V_3Si_{18}^-$. From the structural evolution of $V_3Si_n^-$ (n=3−18), it can therefore be expected that all three V atoms will be encapsulated inside a closed Si cage as the cluster grows even larger.

In order to obtain more bonding information, we examined the average V–Si, Si–Si, and V–V bond lengths of the lowest-energy structures of $V_3Si_{14\text{-}18}^-$ clusters; the results are summarized in Table 1. The average V–Si bond lengths are in a range of 2.60~2.67 Å, which is longer than the average Si–Si bond (2.40~2.51 Å). The shortest V–V ($r_{min\_V\text{-}V}$) bonds are between 2.25 Å and 2.46 Å, which is shorter than the average Si–Si and V–Si bond lengths. In each of $V_3Si_n^-$ cluster, the maximum ($r_{max\_V\text{-}V}$) and middle ($r_{mid\_V\text{-}V}$) V-V bond lengths are longer than the average V–Si and Si–Si bond lengths, respectively, except for $V_3Si_{16}^-$ and $V_3Si_{17}^-$ with the shortest $r_{max\_V\text{-}V}$ and $r_{mid\_V\text{-}V}$, respectively. These results indicate that each $V_3Si_n^-$ (n=14–16,18) cluster possesses one strong V–V bond, while $V_3Si_{17}^-$ has two.

3.3. Electronic Properties of the $V_3Si_n^-$ (n=14−18) clusters

Table 2. Spin multiplicities (SM), relative energies (ΔE), average binding energies (E_b), HOMO-LUMO gaps (E_{HL}), vertical detachment energies (VDEs), and adiabatic detachment energies (ADEs) of the isomers of $V_3Si_n^-$ (n=14−18). The uncertainties in the experimental VDEs and ADEs are given in the parentheses.

Isomer		SM	ΔE (eV)	E_b (eV)	E_{HL}(eV)	Theo. (eV)		Expt. (eV)	
						VDE	ADE	VDE	ADE
$V_3Si_{14}^-$	14A	3	0	4.085	0.320	3.30	3.18	3.40(3)	3.22(3)
		1	0.051	4.082	0.301	3.24	3.12		
	14B	1	0.383	4.062	0.491	3.40	3.22		
	14C	1	0.402	4.060	0.732	3.43	3.33		
$V_3Si_{15}^-$	15A	1	0	4.076	0.540	3.28	3.10	3.38(3)	3.21(3)
		3	0.235	4.063	0.539	3.04	2.86		
	15B	1	0.080	4.070	0.622	3.45	3.31		
		3	0.481	4.049	0.351	3.04	2.90		
	15C	1	0.327	4.056	0.708	3.51	3.44		
$V_3Si_{16}^-$	16A	1	0	4.090	0.520	3.53	3.51	3.65(3)	3.35(3)
		3	0.328	4.073	0.429	3.20	3.18		
	16B	1	0.057	4.087	0.598	3.65	3.49		
		3	0.325	4.073	0.567	3.38	3.22		
	16C	3	0.549	4.060	0.390	3.27	3.21		
$V_3Si_{17}^-$	17A	1	0	4.088	0.804	3.44	3.33	3.53(3)	3.40(3)

		3	0.590	4.059	0.536	2.85	2.74		
	17B	1	0.020	4.088	0.390	3.66	3.58		
		3	0.327	4.072	0.595	3.35	3.25		
	17C	1	0.170	4.080	0.689	3.53	3.37		
	18A	1	0	4.111	0.534	3.67	3.57		
$V_3Si_{18}^-$	18B	1	0.456	4.091	0.889	3.51	3.44	3.70(3)	3.49(3)
	18C	3	0.739	4.077	0.189	3.33	3.25		

In order to further confirm the authenticity of the found ground state structures, the VDE extracted from the measured PES were compared with the simulated ones listed in Table 2 and displayed in Figure 3 (a). The results show a maximum deviation of 0.09 eV between the measured and calculated VDEs at size 16, which indicate a good match. The VDE values show even-odd oscillations in a small range of 3.30~3.70 eV.

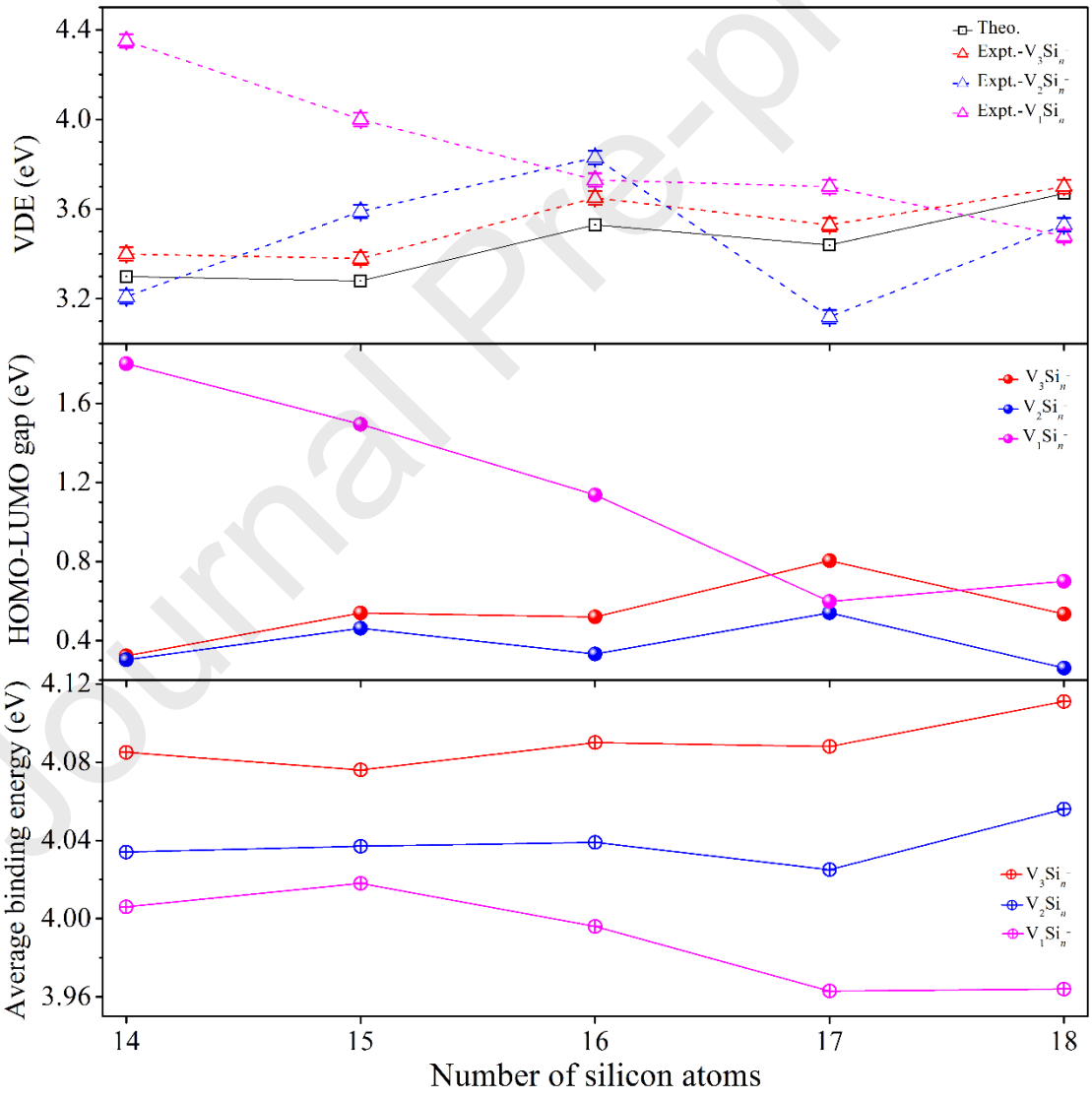

Figure 3. The vertical detachment energies (VDEs), HOMO-LUMO gaps, and average binding energies (E_b) of $V_3Si_n^-$ (n = 14–18) cluster anions are shown as a function of n with comparison of $V_1Si_n^-$ and $V_2Si_n^-$ at the same theory level from references 32 and 38, respectively.

The HOMO-LUMO gap, i.e. the energy difference between the highest occupied molecular orbital (HOMO) and the lowest unoccupied molecular orbital (LUMO), are shown in Figure 3(b). It shows that the HOMO-LUMO gaps of $V_1Si_n^-$(n = 14-16) (see Table S2) are significantly larger than that of $V_2Si_n^-$ and $V_3Si_n^-$.

For a $V_3Si_n^-$ cluster, the stability can be evaluated through the average binding energy (E_b) defined by $E_b(V_3Si_n^-) = [(n\text{-}1)E(Si) + 3E(V) + E(Si^-) – E(V_3Si_n^-)]/(n+3)$, where $E(V_3Si_n^-)$ represents the energy of $V_3Si_n^-$, E(Si), $E(Si^-)$ and E(V) are the total energies of the single Si atom, Si anion, and V atom, respectively. The average binding energy of the ground-state $V_3Si_n^-$ is presented as a function of cluster size in Figure 3(c), it shows prominent odd-even oscillation in the range of 4.076 ~ 4.111 eV/atom. This cannot be an electronic effect as all of the clusters have an even number of electrons, and therefore has to be attributed to the evolution of their geometric structures. It is also noticeable that the enhancement of the stability of silicon clusters with the amount of doped V atoms. The average binding energy of $V_3Si_n^-$ is still far below the bulk cohesive energy of silicon (4.63 eV[62]), but significantly larger than the binding energy of silicon clusters of the same size,[63] which indicates a stability enhancement by the TM doping.

3.4. Magnetic Properties of the $V_3Si_{14}^-$ cluster

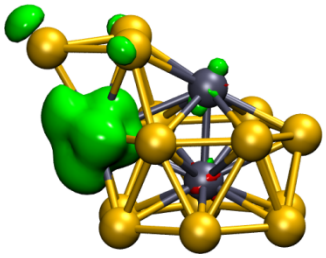

Figure 4. Isosurface mappings of the electron spin density of $V_3Si_{14}^-$ cluster. The isosurface is set to ± 0.005 e/Å^3. Green and red isosurfaces indicate the positive (spin-up) and negative (spin-down) electron spin density, respectively.

Table 3. Mulliken population analysis results of magnetic moments (in units of the Bohr magneton μ_B): magnetic moments of each vanadium atom (μ_V), of their atomic d-orbitals ($\mu_{V\text{-}d}$), and total magnetic moments (μ_T) of $V_3Si_{14}^-$ cluster, with the results of the Hirshfeld population analysis in parentheses for reference. In order to distinguish V atoms which are on the top, bottom and side, they are called V_t, V_b and V_s, respectively.

	atom	μ_V	$\mu_{V\text{-}d}$	μ_T
$V_3Si_{14}^-$	V_t	-0.004 (0.030)	0.007	2 (2)
	V_b	-0.075 (-0.018)	-0.060	
	V_s	1.557 (1.267)	1.400	

To investigate the magnetic properties of $V_3Si_{14}^-$ cluster, the calculated spin-density isosurfaces are displayed in Figure 4. Furthermore, Mulliken population analysis (MPA) was conducted and the results are summarized in Table 3. As shown in Figure 4, the excess alpha electrons marked by the green zones mainly appear around the lateral V atom in $V_3Si_{14}^-$, indicating the major magnetic moments of this V atom. Further MPA analysis indicates that the magnetic moments are dominantly contributed by the d electrons of the V atoms, as one would expect.

4. CONCLUSIONS

In this work, joint PES measurements and DFT calculations were conducted to investigate $V_3Si_n^-$ (n=14–18). The calculated spectra of the lowest-energy structures generated by the global search code are in fair agreement with the experimental results giving evidence that the correct ground state structures have been found. The three V atoms tend to bond with each other, usually forming an acute triangle surrounded by Si atoms which is a nascent nanoscale analogue to bulk phase segregation. For sizes n=14 to 17, the triangle formed by the V atoms resides inside a silicon basket-like structure, while for $V_3Si_{18}^-$ the V_3 triangle is partially encapsulated by a baseball-mitt-like structure. Among these clusters, only $V_3Si_{14}^-$ has a nonzero total magnetic moment, namely a moment of 2 μ_B. Mulliken population analysis shows that this magnetic moment is dominantly contributed by the least encapsulated V atom.

ASSOCIATED CONTENT

Supporting Information

The experimental and simulated photoelectron spectra of $V_3Si_n^-$ (n = 14–18) for the lowest energy structures by using seven functionals are shown in Figure S1. The VDE

values used seven different functional for the ground state of $V_3Si_n^-$ (n = 14–18) are summarize in Table S1. More isomer structures and their simulated photoelectron spectra of $V_3Si_n^-$ (n = 14–18) are depicted in Figure S2 and Figure S3, respectively. The Cartesian coordinates of the low-lying isomers of $V_3Si_n^-$ (n = 14–18) clusters at the BP86/def2-TZVP level can be found in the compressed file xyz.zip.

AUTHOR INFORMATION

Corresponding Author

Lei Ma − Tianjin International Center for Nanoparticles and Nanosystems, Tianjin University, Tianjin 300072, China; Email: lei.ma@tju.edu.cn

Authors

Kai Wang − Tianjin International Center for Nanoparticles and Nanosystems, Tianjin University, Tianjin 300072, China

Guang-Jia Yin − Tianjin International Center for Nanoparticles and Nanosystems, Tianjin University, Tianjin 300072, China

Ze-Zhao Jia − Tianjin International Center for Nanoparticles and Nanosystems, Tianjin University, Tianjin 300072, China

Lin Miao − Tianjin International Center for Nanoparticles and Nanosystems, Tianjin University, Tianjin 300072, China

Hong-Yuan Zhao − Tianjin International Center for Nanoparticles and Nanosystems, Tianjin University, Tianjin 300072, China

Ramiro Moro − Tianjin International Center for Nanoparticles and Nanosystems, Tianjin University, Tianjin 300072, China

Bernd von Issendorff − Fakultät für Physik, Universität Freiburg, D-79104 Freiburg, Germany

Notes

The authors declare no competing financial interest.

ACKNOWLEDGMENTS

This work was supported by the National Natural Science Foundation of China under Grant No. 11774255 and the National R&D Program of China No. 2020YFC2004602.

REFERENCES

(1) Ho, K.-M.; Shvartsburg, A. A.; Pan, B.; Lu, Z.-Y.; Wang, C.-Z.; Wacker, J. G.; Fye J. L.; Jarrold, M. F. Structures of medium-sized Silicon clusters. Nature 1998, **392**, 582-585.

(2) Hoffmann, M. A.; Wrigge, G.; Issendorff, B. v.; Müller, J.; Ganteför G.; Haberland, H. Ultraviolet photoelectron spectroscopy of Si_4^- to Si_{1000}^-. Eur. Phys. J. D 2001, **16**, 9-11.

(3) Jarrold, M. F.; Constant, V. A. Silicon Cluster Ions: Evidence for a Structural Transition. Phys. Rev. Lett. 1991, **67**, 2994-2997.

(4) Müller, J.; Liu, B.; Shvartsburg, A. A.; Ogut, S.; Chelikowsky, J. R.; Siu, K. W. M.; Ho, K.-M.; Gantefor, G. Spectroscopic Evidence for the Tricapped Trigonal Prism Structure of Semiconductor Clusters. Phys. Rev. Lett. 2000, **85**, 1666-1669.

(5) Guliamov, O.; Kronik, L.; Jackson, K. A. Photoelectron spectroscopy as a structural probe of intermediate size clusters. J. Chem. Phys. 2005, **123**, 204312.

(6) Goedecker, S.; Hellmann, W.; Lenosky, T. Global Minimum Determination of the Born-Oppenheimer Surface within Density Functional Theory. Phys. Rev. Lett. 2005, **95**, 055501.

(7)Yoo, S.; Zeng, X. C. Motif Transition in Growth Patterns of Small to Medium-Sized Silicon Clusters. Angew. Chem. 2005, **117**, 1515-1518.

(8) Ding, L. P.; Zhang, F. H.; Zhu, Y. S.; Lu, C.; Kuang, X. Y.; Lv, J.; Shao, P. Understanding the structural transformation, stability of medium-sized neutral and charged silicon clusters. Sci. Rep. 2015, **5**, 15951.

(9) Xue, W.; Liang, X.; Du, Q.; Zhao, J.; Chen, M.; Miao, L.; Wang, J.; Yin, G.; Ma, L.; King, R. B.; et al. Medium-sized Si_n^- (n=14−20) clusters: a combined study of photoelectron spectroscopy and DFT Calculations. J. Phys.: Condens. Matter 2018, 30, 354002.

(10) Jarrold, M. F.; Bower, J. E. Mobilities of silicon cluster ions: The reactivity of silicon sausages and spheres. J. Chem. Phys. 1992, **96**, 9180-9190.

(11) Röthlisberger, U.; Andreoni, W.; Parrinello, M. Structure of Nanoscale Silicon Clusters. Phys. Rev. Lett. 1994, **72**, 665-668.

(12) Rata, I.; Shvartsburg, A. A.; Horoi, M.; Frauenheim, T.; Siu, K. W. M.; Jackson, K. A. Single-Parent Evolution Algorithm and the Optimization of Si Clusters. Phys. Rev. Lett. 2000, **85**, 546-549.

(13) Kumar, V.; Kawazoe, Y. Metal-Encapsulated Fullerenelike and Cubic Caged Clusters of Silicon. Phys. Rev. Lett. 2001, 87, 045503.

(14) Kumar, V. Alchemy at the nanoscale: Magic heteroatom clusters and assemblies. Comp. Mater. Sci. 2006, **36**, 1-11.

(15) Koyasu, K.; Akutsu, M.; Mitsui, M.; Nakajima, A. Selective Formation of MSi_{16} (M=Sc, Ti, and V), J. Am. Chem. Soc. 2005, **127**, 4998-4999.

(16) Nakajima, A. Study on Electronic Properties of Composite Clusters toward Nanoscale Functional Advanced Materials. Bull. Chem. Soc. Jpn. 2013, 86, 414−437.

(17) Neukermans, S.; Wang, X.; Veldeman, N.; Janssens, E.; Silverans, R. E.; Lievens, P. Mass spectrometric stability study of binary MS_n clusters (S=Si, Ge, Sn, Pb, and M=Cr, Mn, Cu, Zn). Int. J. Mass Spectrom. 2006, 252, 145−150.

(18) Jena, P.; Sun, Q. Super Atomic Clusters: Design Rules and Potential for Building Blocks of Materials. Chem. Rev. 2018, 118, 5755−5870.

(19) Koyasu, K.; Atobe, J.; Furuse, S.; Nakajima, A. Anion photoelectron spectroscopy of transition metal- and lanthanide metal-silicon clusters: MSi_n^- (n=6-20) A. J. Chem. Phys. 2008, 129, 214301.

(20) Zheng, W.; Nilles, J. M.; Radisic, D.; Bowen, K. H. Photoelectron spectroscopy of chromium-doped silicon cluster anions. J. Chem. Phys. 2005, **122**, 071101.

(21) Guo, L.-J.; Liu, X.; Zhao, G.-F.; Luo, Y.-H. Computational investigation of $TiSi_n$ (n = 2−15) clusters by the density-functional theory. J. Chem. Phys. 2007, **126**, 234704.

(22) Kawamura, H.; Kumar, V.; Kawazoe, Y. Growth, magic behavior, and electronic and vibrational properties of Cr-doped Si clusters. Phys. Rev. B 2004, **70**, 245433.

(23) Kumar, V.; Kawazoe, Y. Magic behavior of $Si_{15}M$ and $Si_{16}M$ (M=Cr, Mo, and W) clusters. Phys. Rev. B 2002, **65**, 073404.

(24) Torres, M. B.; Fernández, E. M.; Balbás, L. C. Theoretical study of isoelectronic Si_nM clusters (M=Sc^- , Ti, V^+; n=14−18). Phys. Rev. B 2007, 75, 205425.

(25) Ma, L.; Zhao, J.; Wang, J.; Wang, B.; Lu, Q.; Wang, G. Growth behavior and magnetic properties of Si_nFe (n=2–14) clusters. Phys. Rev. B 2006, **73**, 125439.

(26) Ma, L.; Zhao, J.; Wang, J.; Lu, Q.; Zhu, L.; Wang, G. Structure and electronic properties of cobalt atoms encapsulated in Si_n (n = 1–13) clusters. Chem. Phys. Lett. 2005, **411**, 279-284.

(27) Ren, Z.-Y.; Li, F.; Guo, P.; Han, J.-G. A computational investigation of the Ni-oped Si_n (n=1-8) clusters by a density functional method. J. Mol. Stru.: THEOCHEM 2005, **718**, 165-173.

(28) Kong, X.; Xu, H. G.; Zheng, W. Structures and magnetic properties of $CrSi_n^-$ (n = 3−12) clusters: Photoelectron spectroscopy and density functional calculations. J. Chem. Phys. 2012, 137, 064307.

(29) Xu, H. G.; Wu, M. M.; Zhang, Z. G.; Yuan, J.; Sun, Q.; Zheng, W. Photoelectron spectroscopy and density functional calculations of $CuSi_n^-$ (n = 4−18) clusters. J. Chem. Phys. 2012, 136, 104308.

(30) Lu, S. J.; Cao, G. J.; Zheng, W. J. The structural and electronic properties of $NbSi_n^{-/0}$ (n = 3−12) clusters: anion photoelectron spectroscopy and ab initio calculations. Nanoscale 2016, 8, 19769−19778.

(31) Kong, X. Y.; Deng, X. J.; Xu, H. G.; Yang, Z.; Xu, X. L.; Zheng, W. J. Photoelectron spectroscopy and density functional calculations of $AgSi_n^-$ (n = 3−12) clusters. J. Chem. Phys. 2013, 138, 244312.

(32) Wang, K.; Jia, Z.-Z.; Fan, Z.; Zhao, H.-Y.; Yin, G.-J.; Moro, R.; Issendorff, B. von ; Ma, L. Structures and electronic properties of VSi_n^- (n = 14–20) clusters: a combined experimental and density functional theory study. Phys. Chem. Chem. Phys. 2022, 24, 8839 – 8845.

(33) Wang, K.; Zhao, H.-Y.; Miao, L.; Jia, Z.-Z.; Yin, G.-J.; Zhu, X.-D.; Moro, R.; Issendorff, B. von ; Ma, L. Photoelectron Spectroscopy and Density Functional Investigation of the Structural Evolution, Electronic, and Magnetic Properties of $CrSi_n^-$ (n = 14−18) Clusters. J. Phys. Chem. A 2022, 126, 1329−1335.

(34) Zhang, L.-J.; Yang, B.; Li, D.-Z.; Farooq, U.; Xu, X.-L.; Zheng, W.-J.; and Xu, H.-G. Appearance of V-encapsulated tetragonal prism motifs in VSi10− and VSi11− clusters. Phys. Chem. Chem. Phys., 2020, 22, 22989.

(35) Xu, H. G.; Zhang, Z. G.; Feng, Y.; Yuan, J.; Zhao, Y.; Zheng, W. Vanadium-doped small silicon clusters: Photoelectron spectroscopy and density-functional calculations. Chem. Phys. Lett. 2010, 487, 204−208.

(36) Li, C.; Chen, W.; Cui, Y.; Li, W.; Li, G.; Ma, Y.; Li, H.; Ren, B.; Hu, Y.; Structures, stabilities and electronic properties of the bimetal V_2-doped Si_n (n = 1−10) clusters: a density functional investigation Eur. Phys. J. D, 2020, 74, 111.

(37) Xu, H. G.; Zhang, Z. G.; Feng, Y.; Zheng, W. Photoelectron spectroscopy and density-functional study of $Sc_2Si_n^-$ (n= 2−6) Clusters. Chem. Phys. Lett. 2010, 498, 22−26.

(38) Wang, K.; Yin, G.-J.; Jia, Z.-Z.; Miao, L.; Moro, R.; Issendorff, B. von ; Ma, L. Anion photoelectron spectroscopy and density functional theory study of $TM_2Si_n^-$ (TM = V, Cr; n = 14–20) clusters. Phys. Chem. Chem. Phys. 2022, 24, 18321-18330.

(39) Xu, H.-G.; Kong, X.-Y.; Deng, X.-J.; Zhang, Z.-G.; Zheng, W.-J. Smallest fullerene-like silicon cage stabilized by a V_2 unit. J. Chem. Phys. 2014, **140**, 024308.

(40) Yang, B.; Xu, H.; Xu, X.; Zheng, W. Photoelectron Spectroscopy and Theoretical Study of $Cr_nSi_{15-n}^-$ (n=1−3): Effects of Doping Cr Atoms on the Structural and Magnetic Properties. J. Phys. Chem. A 2018, 122, 9886−9893.

(41) Huang, X.; Xu, H. G.; Lu, S.; Su, Y.; King, R. B.; Zhao, J.; Zheng, W. Discovery of a silicon-based ferrimagnetic wheel structure in $V_xSi_{12}^-$ (x=1−3) clusters: photoelectron spectroscopy and density functional theory investigation. Nanoscale 2014, 6, 14617−14621.

(42) Huang, X.; Lu, S. J.; Liang, X.; Su, Y.; Sai, L.; Zhang, Z. G.; Zhao, J.; Xu, H. G.; Zheng, W. Structures and Electronic Properties of $V_3Si_n^-$ (n = 3−14) Clusters: A Combined Ab Initio and Experimental Study. J. Chem. Phys. C 2015, 119, 10987−10994.

(43) Ma, L.; Issendorff, B. v.; Aguado, A. Photoelectron spectroscopy of cold aluminum cluster anions: Comparison with density functional theory results. J. Chem. Phys. 2010, 132, 104303.

(44) Wang, K.; Jia, Z. –Z.; Wang, R. -Y.; Zhu, X.-D.; Moro, R.; Ma, L. $TMGe_{8-17}^-$ (TM= Ti, Zr, Hf, V, Nb, Ta) clusters: group determined properties. Eur. Phys. J. Plus 2022, 137, 949.

(45) Wang, K.; Miao, L.; Jia, Z.-Z.; Wang, R. -Y.; Yin, G.J.; Zhu, X.-D.; Moro, R.; Ma, L. Structural evolution and electronic properties of pure and semiconductor atom doped In clusters: In_n^-, In_nSi^-, and In_nGe^- (n = 3–16). J. Comput. Chem. 2022, 43,1978–1984.

(46) Neese, F. The ORCA program system. WIREs Comput. Mol. Sci. 2012, 2, 73−78.

(47) Neese, F. Software update: the ORCA program system, version 4.0. WIREs Comput. Mol. Sci. 2017, 8, e1327.

(48) Perdew, J. P. Density-functional approximation for the correlation energy of the inhomogeneous electron gas. Phys. Rev. B 1986, 33, 8822–8824.

(49) Weigend, F.; Ahlrichs, R. Balanced Basis Sets of Split Valence, Triple Zeta Valence and Quadruple Zeta Valence Quality for H to Rn: Design and Assessment of Accuracy. Phys. Chem. Chem. Phys. 2005, 7, 3297−3305.

(50) Weigend, F. Accurate Coulomb-fitting basis sets for H to Rn. Phys. Chem. Chem. Phys. 2006, 8, 1057−1065.

(51) Rappoport, D.; Furche, F. Property-optimized Gaussian basis sets for molecular response calculations.J. Chem. Phys. 2010, 133, 134105.

(52) Perdew, J. P.; Burke, K.; Ernzerhof, M. Generalized Gradient Approximation Made Simple. Phys. Rev. Lett. 1996, 77, 3865.

(53) Becke, A. D. Density-functional exchange-energy approximation with correct asymptotic behavior. Phys. Rev. A 1988, 38, 3098−3100.

(54) Lee, C.; Yang, W.; Parr, R. G. Development of the Colle-Salvetti Correlation-Energy Formula into a Functional of the Electron Density. Phys. Rev. B 1988, 37, 785−789.

(55) Adamo, C.; Barone, V. Toward reliable density functional methods without adjustable parameters: The PBE0 model. J. Chem. Phys. 1999, 110, 6158.

(56) Tao, J.; Perdew, J. P.; Staroverov, V. N.; Scuseria, G. E. Climbing the Density Functional Ladder: Nonempirical Meta–Generalized Gradient Approximation Designed for Molecules and Solids. Phys. Rev. Lett. 2003, 91, 146401.

(57) Staroverov, V. N.; Scuseria, G. E.; Tao, J.; Perdew, J. P. Comparative assessment of a new nonempirical density functional: Molecules and hydrogen-bonded complexes. J. Chem. Phys. 2003, 119, 12129.

(58) Becke, A. D. Density Functional Thermochemistry. III. The Role of Exact Exchange. J. Chem. Phys. 1993, 98, 5648.

(59) Akola, J.; Manninen, M.; Häkkinen, H.; Landman, U.; Li, X.; Wang, L. S. Photoelectron spectra of aluminum cluster anions: Temperature effects and ab initio simulations. Phys. Rev. B 1999, 60, R11297−R11300.

(60) Humphrey, W.; Dalke, A.; Schulten, K. VMD: Visual molecular dynamics. J. Mol. Graph. 1996, 14, 33−38.

(61) Lu, T.; Chen, F. Multiwfn: A multifunctional wavefunction analyzer. J. Comput. Chem. 2012, 33, 580−592.

(62) Kittel, C. Introduction to Solid State Physics, Wiley, New York, 1996.

(63) Qin, W.; Lu, W.-C.; Zhao, L.-Z.; Zang, Q.-J.; Wang, C. Z.; Ho, K. M. Stabilities and fragmentation energies of Si_n clusters (n = 2–33). J. Phys.: Condens. Matter **2009, 21**, 455501.

TOC Graphic

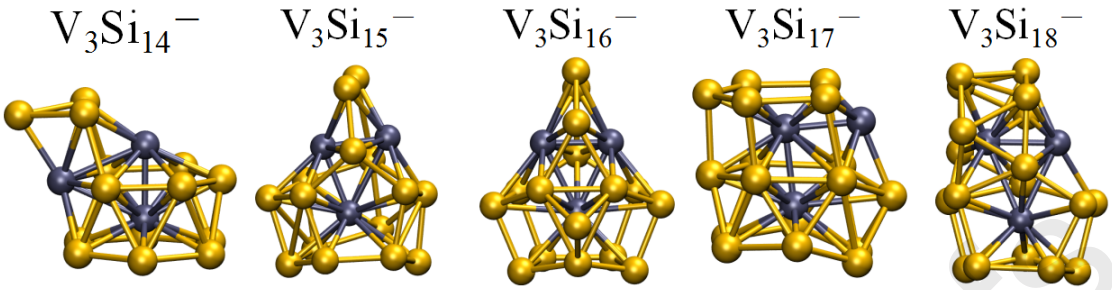

Credit Author Statement

Kai Wang: Methodology, Investigation, Data curation, Writing–original draft preparation.

Guang-Jia Yin: Methodology, Investigation, Data curation.

Ze-Zhao Jia: Investigation, Data curation.

Lin Miao: Investigation, Data curation.

Hong-Yuan Zhao: Investigation, Data curation.

Ramiro Moro: Writing-review & editing.

Bernd von Issendorff: Validation, Writing-review & editing.

Lei Ma: Conceptualization, Supervision, Methodology, Validation, Writing- review & editing, Funding acquisition, project administration.

Declaration of interests

☒ The authors declare that they have no known competing financial interests or personal relationships that could have appeared to influence the work reported in this paper.

☐The authors declare the following financial interests/personal relationships which may be considered as potential competing interests:

Highlights

- The low-lying isomers of $V_3Si_n^-$ (n=14–18) clusters were globally searched by using a homemade genetic algorithm code coupled with the density functional theory calculations.
- The ground-state structures of these clusters were confirmed by the comparison of the simulated and experimental photoelectron spectra.
- The three V atoms tend to bond with each other, usually forming an acute triangle surrounded by Si atoms which is a nascent nanoscale analogue to bulk phase segregation.
- Among these clusters, only $V_3Si_{14}^-$ has a nonzero total magnetic moment, namely a moment of 2 μ_B.

Graphical Abstract

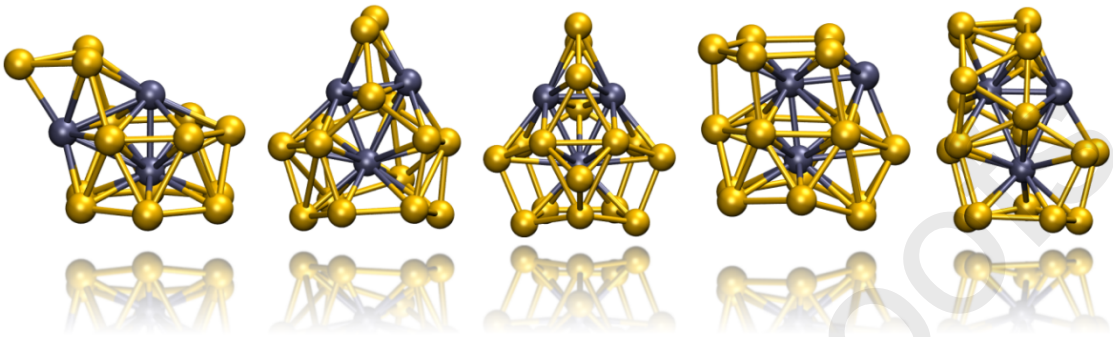

The structural evolution and electronic properties of $V_3Si_n^-$ (n=14–18) were investigated by the combination of high-resolution photoelectron spectroscopy (PES) measurements and density functional theory calculations. The ground-state structures of these clusters were confirmed by the comparison of the simulated and experimental spectra. The three V atoms tend to bond with each other, usually forming an acute triangle surrounded by Si atoms which is a nascent nanoscale analogue to bulk phase segregation.